

Electrical Characteristics of an Optically Controlled N-Channel AlGaAs/GaAs/InGaAs Pseudomorphic HEMT

Dong Myong Kim, Sang Ho Song, Hwe Jong Kim, and Kwang Nham Kang

Abstract— Electrical characteristics of an n-channel $\text{Al}_{0.3}\text{Ga}_{0.7}\text{As}/\text{GaAs}/\text{In}_{0.13}\text{Ga}_{0.87}\text{As}$ pseudomorphic HEMT (PHEMT) with $L_g = 1 \mu\text{m}$ on GaAs are characterized under optical input (P_{opt}). Gate leakage and drain current have been analyzed as a function of V_{GS} , V_{DS} , and P_{opt} . We observed monotonically increasing gate leakage current due to the energy barrier lowering by the optically induced photovoltage, which means that gate input characteristics are significantly limited by the photovoltaic effect. However, we obtained a strong nonlinear photoresponsivity of the drain current, which is limited by the photoconductive effect. We also proposed a device model with an optically induced parasitic $\text{Al}_{0.3}\text{Ga}_{0.7}\text{As}$ MESFET parallel to the $\text{In}_{0.13}\text{Ga}_{0.87}\text{As}$ channel PHEMT for the physical mechanism in the drain current saturation under high optical input power.

Index Terms— FET, GaAs, HEMT, optoelectronics, photodetector.

I. INTRODUCTION

AN INCREASING attention has been created on the photonic microwave systems due to their applications in high-performance communication systems. Significant progress has been also reported in high-speed photodetection systems on Si, GaAs, and InP substrates [1]–[6]. It is well known that there are two main physical mechanisms, photoconductive effect and photovoltaic effect, in semiconductor devices under optical illumination. They are all caused by photogenerated excess electron-hole-pairs and closely related with each other. Some of photogenerated excess carriers contribute to the change of channel conductivity (such as photoconductivity in bulk photoconductors) while others contribute to the change of depletion region under the gate (such as photovoltaic effect or effective built-in voltage change in solar cells or photodiodes which use pn junctions). However, it is very hard to distinguish one effect from the other. As far as we know, photoconductivity change appears as a change in the channel current due to increased carrier density in the channel layer. On the other hand, the photovoltaic effect appears as a change in the effective built-in junction voltage and thus gate junction capacitance which

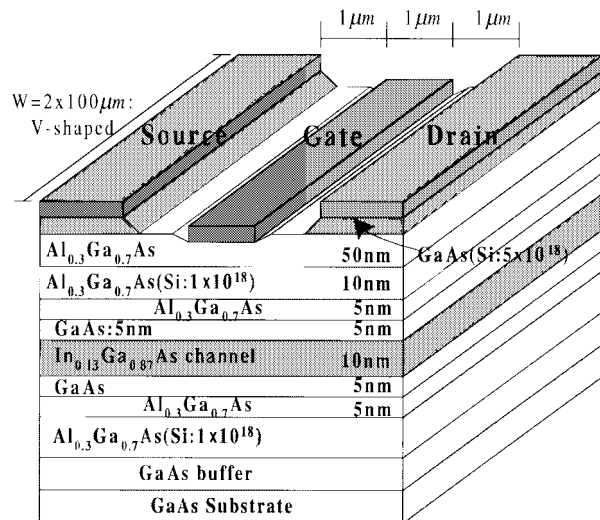


Fig. 1. A cross-sectional structure of an optically controlled N-channel AlGaAs/GaAs/InGaAs PHEMT (V-shaped dual gate) with $L_G = 1 \mu\text{m}$, $L_{GS} = L_{GD} = 1 \mu\text{m}$, and $W = 2 \times 100 \mu\text{m}$.

affects high-frequency characteristics of devices under optical illumination.

The photoconductive effect on the surface-illuminated field effect transistors is known to be very fast but small contribution to the change in the drain current while the photovoltaic effect is known to be relatively slow but significant contribution to the change in the drain current under optical illumination [6]. Concerning physical mechanisms in electrical characteristics of optically controlled high electron mobility transistors (HEMT's), which has different optoelectronic responsivity and mechanisms in MESFET's, it is still necessary to figure out key factors in the design and optimization of HEMT's for high-performance optoelectronic detectors.

In this paper, optically controlled electrical characteristics of an n-channel $\text{Al}_{0.3}\text{Ga}_{0.7}\text{As}/\text{GaAs}/\text{In}_{0.13}\text{Ga}_{0.87}\text{As}$ pseudomorphic HEMT(PHEMT) are reported and analyzed. In particular, a parasitic $\text{Al}_{0.3}\text{Ga}_{0.7}\text{As}$ MESFET is included as a dominant photoresponsive element over the pseudomorphic $\text{In}_{0.13}\text{Ga}_{0.87}\text{As}$ HEMT under high optical input.

II. PHOTONIC CURRENT-VOLTAGE CHARACTERISTICS OF THE PHEMT

The epitaxial layers of the PHEMT were grown on S.I. GaAs substrate by a GSMBE. A symmetrical $\text{Al}_{0.3}\text{Ga}_{0.7}\text{As}/\text{GaAs}/\text{In}_{0.13}\text{Ga}_{0.87}\text{As}$ double heterojunction

Manuscript received July 1, 1998; revised October 13, 1998. This work was supported in part by KOSEF Contract 981-0098-029-2 and Korea Ministry of Information and Communication.

D. M. Kim is with the School of Electrical Engineering, Kookmin University, Seoul 136-702, Korea (e-mail: dmkim@kmu.kookmin.ac.kr).

S. H. Song is with Samsung Electronics, Kyungki 449-900, Korea.

H. J. Kim and K. N. Kang are with the Photonics Research Center, Korea Institute of Science and Technology, Seoul 130-760, Korea.

Publisher Item Identifier S 0741-3106(99)01056-3.

In_{0.13}Ga_{0.87}As quantum well has been grown for better photoresponsivity with a high-density 2-DEG's and an improved mobility. As shown in Fig. 1, GaAs layers are expected to have an elevated contribution to improved photoconductivity. Symmetrical structure is also expected to have improved transport with compensated Coulombic scattering between 2-DEG's and ionized donors in Al_{0.3}Ga_{0.7}As layers. From the Hall measurement at 300 K, we obtained $\mu_n = 5000[\text{cm}^2/\text{Vs}]$ and $n_s = 1.2 \times 10^{12} [\text{cm}^{-2}]$ for the two-dimensional electron gas (2-DEG). A V-shaped gate structure ($L_G = 1 \mu\text{m}$, $L_{GS} = L_{GD} = 1 \mu\text{m}$, $W = 200 \mu\text{m}$) has been fabricated for better controllability and photosensitivity of the PHEMT under optical control.

Electrical performance of the PHEMT with a V-shaped gate has been characterized as a function of gate voltage (V_{GS}), drain voltage (V_{DS}), and optical power (P_{opt}). P_{opt} -dependent electrical characteristics are measured on wafer by combining the HP-4156A and a laser diode module with $\lambda = 0.83 \mu\text{m}$. We obtained a saturated drain current $I_{DSS} = 12.0 \text{ mA}$ (23.5mA), a pinchoff voltage $V_P = -0.9 \text{ V}$ (-1.2 V), a maximum extrinsic transconductance $g_{m(\text{max})} = 130 \text{ mS/mm}$ (155 mS/mm), and an output resistance $r_{ds} = 760 \Omega$ ($>40 \text{ k}\Omega$) under $P_{\text{opt}} = 0 \text{ mW}$ (20 mW), respectively. Characterized n-channel PHEMT shows significant improvements in the output resistance and the maximum transconductance due to increased 2-DEG's and reduced parasitic resistances under optical illumination.

The gate current (I_G) is shown in Fig. 2 as a function of V_{GS} , V_{DS} , and P_{opt} . The gate leakage increases monotonically with increasing reverse gate voltage for given V_{DS} and P_{opt} while it is almost independent of V_{DS} for given V_{GS} and P_{opt} . The gate current increases sharply with increasing P_{opt} for given V_{GS} and V_{DS} . $I_G - (V_{DS}, V_{GS})$ curves look a parallel shift with increasing P_{opt} due to the photovoltaic effect and an optically generated photovoltage (V_{opt}). Considering the strong dependence of $I_G - (V_{DS}, V_{GS})$ on P_{opt} , the gate leakage current is expected to be mainly caused by the photovoltaic effect, which results in reduced energy barrier against photogenerated carriers by the amount of the qV_{opt} . The gate current can be described by $I_G = I_{G_0}(V_{GS}, V_{DS}) e^{\Delta E/kT} = I_{G_0}(V_{GS}, V_{DS}) e^{qV_{\text{opt}}/V_{th}}$ considering thermionic emission-dominant current conduction, where I_{G_0} and ΔE are the gate current under $P_{\text{opt}} = 0$ and the energy barrier reduction by the photovoltaic effect, respectively. This agrees well with experimental observation of P_{opt} -dependent gate current.

The drain current (I_D) is also characterized as a function of V_{GS} , V_{DS} , and P_{opt} . Contrary to $I_G - (V_{DS}, V_{GS})$ on P_{opt} , the drain current shows strong dependence on V_{GS} for given V_{DS} and P_{opt} as shown in Fig. 3. I_D sharply increases at low P_{opt} while it saturates at high P_{opt} under specific V_{GS} and V_{DS} . The shape of $I_D - (V_{DS}, V_{GS})$ curves for all optical inputs is similar to that under $P_{\text{opt}} = 0$. $I_D - (V_{DS}, V_{GS})$ of the PHEMT is predominantly controlled by the photoconductive effect with optically generated excess electrons while the gate current is determined by the photovoltaic effect. However, the saturated drain current I_{DSS} shows almost constant over $P_{\text{opt}} \geq 3 \text{ mW}$, which is significantly different from the gate current under high

P_{opt} . Concerning the limited I_{DSS} and transconductance over $P_{\text{opt}} \geq 3 \text{ mW}$, a parallel conduction by N-type Al_{0.3}Ga_{0.7}As donor layers, which has significantly low electron mobility due to high density of ionized donor atoms in the wide bandgap semiconductor, is believed to be the main cause. Because optically generated excess carriers induce a large photovoltage, reduced effective negative V_{GS} makes incomplete transfer of electrons from the Al_{0.3}Ga_{0.7}As layers to the channel. Thus, partially depleted Al_{0.3}Ga_{0.7}As layers form a parasitic MESFET, which has poor channel conductance as well as large parasitic source and drain resistances (R_s, R_d), parallel to the high-performance In_{0.13}Ga_{0.87}As-channel PHEMT shown as an inset in Fig. 3. Including a current through the parasitic MESFET, therefore, total drain current I_D can be described by $I_D = I_{D,\text{HEMT}}(P_{\text{opt}}) + I_{D,\text{MESFET}}(P_{\text{opt}})$, where $I_{D,\text{HEMT}}$ and $I_{D,\text{MESFET}}$ are current components through the In_{0.13}Ga_{0.87}As-channel and the partially depleted Al_{0.3}Ga_{0.7}As layer, respectively. Under low P_{opt} , the drain current is mainly controlled by the In_{0.13}Ga_{0.87}As-channel PHEMT and strongly depends on P_{opt} . Thus, I_D can be obtained from $I_D|_{\text{low}P_{\text{opt}}} \approx I_{D,\text{HEMT}}(P_{\text{opt}})$. Under $P_{\text{opt}} \geq 3 \text{ mW}$, however, the drain current consists of a current through the In_{0.13}Ga_{0.87}As-channel PHEMT, which is almost independent of P_{opt} above $P_{\text{opt}} \geq 3 \text{ mW}$, and a current through the partially depleted parasitic Al_{0.3}Ga_{0.7}As MESFET, which still depends strongly on the P_{opt} . Thus, the total drain current under high P_{opt} can be described by $I_D|_{\text{high}P_{\text{opt}}} = I_{D,\text{HEMT}}(\text{sat}) + I_{D,\text{MESFET}}(P_{\text{opt}})$. Even with increased carrier density in the Al_{0.3}Ga_{0.7}As layer at high P_{opt} , the change in the I_D is small due to extremely low mobility in heavily doped ($1 \times 10^{18} \text{ cm}^{-3}$) Al_{0.3}Ga_{0.7}As layers. Overall characteristics of the PHEMT are controlled by the high-performance In_{0.13}Ga_{0.87}As channel HEMT under low P_{opt} . However, the poor performance parasitic Al_{0.3}Ga_{0.7}As MESFET plays a dominant role and limits both the saturated drain current and transconductance under high optical power. This parasitic MESFET phenomenon can be also observed with limited drain saturation current under large positive V_{GS} in n-channel HEMT's [7], [8].

In the saturation mode, the channel length modulation and the output resistance are significantly improved under optical input, as shown in Fig. 3. Increased output resistance (r_{ds}) and suppressed channel length modulation are mainly due to the increased channel conductivity with optically generated excess carriers. Improved r_{ds} under optical illumination can be modeled via a channel length modulation parameter (λ). For drain voltages with $V_{DS} > V_{D\text{sat}}$, the channel length modulation parameter λ is related to the saturated drain current described by

$$\begin{aligned} I_{D\text{sat}} &= I_{DSS}(1 + \lambda V_{DS}) \\ &= I_{DSS} \left[1 + \lambda_o \left(\frac{n_{\text{chlo}}}{n_{\text{chlo}} + \delta n(P_{\text{opt}})} \right) V_{DS} \right] \\ &\quad \text{for } V_{DS} > V_{D\text{sat}} \end{aligned} \quad (1)$$

where $V_{D\text{sat}}$ is the drain saturation voltage, I_{DSS} is the saturated drain current without channel length modulation, and λ_o is defined as λ under $P_{\text{opt}} = 0$. Combining optically gener-

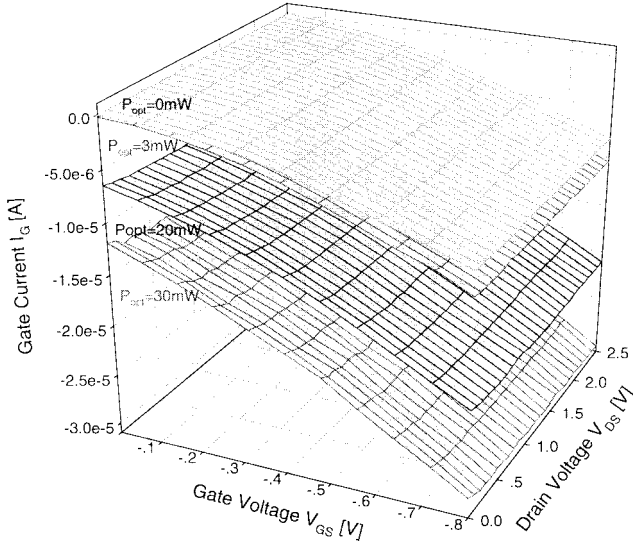


Fig. 2. The optical power (P_{opt})-dependent gate leakage current (I_G) as a function of the gate voltage (V_{GS}) and the drain voltage (V_{DS}). Gate current monotonically increases with increasing P_{opt} .

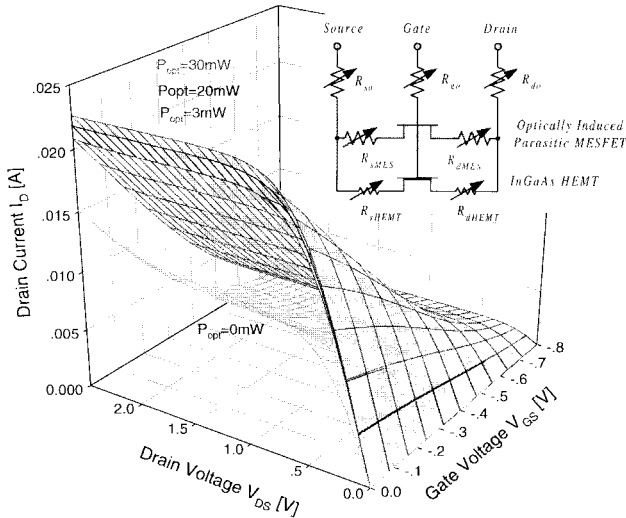


Fig. 3. Optical power (P_{opt})-dependent drain current (I_D) as a function of the gate voltage (V_{GS}) and the drain voltage (V_{DS}) with an inset as an equivalent circuit for parallel conduction due to $\text{Al}_{0.3}\text{Ga}_{0.7}\text{As}$ donor layer. Under high P_{opt} , drain current is saturated over $P_{\text{opt}} \geq 3$ mW.

ated excess carriers $\delta n(P_{\text{opt}})$ into channel length modulation parameter, the output resistance r_{ds} can be described by

$$\begin{aligned} r_{\text{ds}}|_{\text{sat}} &\equiv 1/(dI_D/dV_{\text{DS}})|_{\text{sat}} = \frac{1}{I_{\text{DSS}}\lambda_o} \left(1 + \frac{\delta n(P_{\text{opt}})}{n_{\text{cho}}} \right) \\ &= r_{\text{dso}} \left(1 + \frac{\delta n(P_{\text{opt}})}{n_{\text{cho}}} \right), \end{aligned} \quad (2)$$

where r_{dso} is an output resistance under $P_{\text{opt}} = 0$. Increasing optical power and thus, photo-generated excess carriers, the output resistance can be significantly improved. This simple model agrees well with experimental observations ($r_{\text{dso}} \sim 760 \Omega$ and $r_{\text{ds}}(30\text{mW}) > 40 \text{ k}\Omega$) under high optical input as shown in Fig. 3.

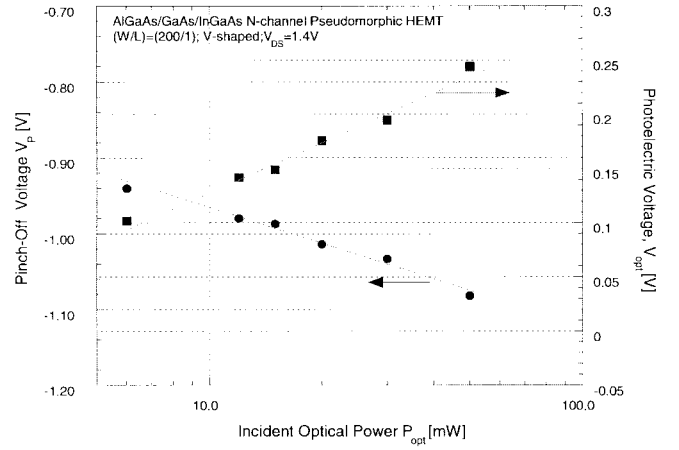


Fig. 4. Variation of pinchoff voltage (V_P) and optically induced photovoltage (V_{opt}) measured at $V_{\text{DS}} = 1.4$ V as a function of optical power (P_{opt}).

Pinchoff voltage V_P and photovoltage ($V_{\text{opt}} = |V_P - V_{p0}|$) were also extracted as a function of P_{opt} in the saturation mode of operation. Without optical input, the pinchoff voltage was measured to be $V_{p0} = -0.84$ V by the quadratic extrapolation method at $V_{\text{DS}} = 1.4$ V. We obtained pinchoff voltages ranging from $V_P = -0.94$ to -1.08 V, which can be converted into photovoltages from $V_{\text{opt}} = 0.10$ – 0.24 V, with $P_{\text{opt}} = 6$ – 50 mW, as shown in Fig. 4. Thus, optical power- and structure-dependent V_{opt} can be obtained from the optically induced excess charge (Q_{opt}) and the gate capacitance (C_g) as

$$V_{\text{opt}} = \frac{Q_{\text{opt}}}{C_g} \cong \frac{qd_{\text{sp}}n_{\text{cho}}}{2\varepsilon_{\text{sp}}} (\sqrt{1 + \alpha' P_{\text{opt}}} - 1), \quad (3)$$

where d_{sp} , ε_{sp} , and α' denote a distance from the gate to the channel, an average dielectric constant, and absorption-related parameter, respectively. This P_{opt} -dependent photovoltage agrees well with experimental observation as shown in Fig. 4. We also note that $\Delta I_D = 4.4$ mA is a significant increase and agrees well with current–voltage characteristics with $V_{\text{opt}} = 0.17$ V, $g_m = 130$ mS/mm, $P_{\text{opt}} = 20$ mW, and $W = 200 \mu\text{m}$. This photovoltaic effect will change high-frequency characteristics of PHEMT's with variations in gate capacitances in conjunction with photoconductive effect (ΔI_D and Δg_m) under optical illumination.

III. CONCLUSION

Electrical characteristics of an n-channel $\text{Al}_{0.3}\text{Ga}_{0.7}\text{As}/\text{GaAs}/\text{In}_{0.13}\text{Ga}_{0.87}\text{As}$ PHEMT are characterized under optical input. We observed monotonically increasing gate leakage due to the energy barrier lowering by the photovoltaic effect. However, we obtained strong nonlinear photoresponsivity of the drain current, which is limited by the photoconductive effect, under optical input. We also observed saturation of the drain current under high P_{opt} , which is believed to be due to the parallel conduction by the parasitic $\text{Al}_{0.3}\text{Ga}_{0.7}\text{As}$ MESFET with poor electrical performance. We also proposed a new device model with an optically induced parasitic $\text{Al}_{0.3}\text{Ga}_{0.7}\text{As}$ MESFET parallel to the

$\text{In}_{0.13}\text{Ga}_{0.87}\text{As}$ channel PHEMT for the physical mechanism of the current saturation under high optical input power.

REFERENCES

- [1] Y. K. Fang, K. H. Lee, K. H. Wu, and C. Y. Tsao, "An integrated PIN/MISS OEIC for high current photoreceiver applications," *IEEE Trans. Electron Devices*, vol. 44, pp. 34–38, Jan. 1997.
- [2] K. Ayadi, G. Bickel, M. Kujik, P. Heremans, G. Borghs, and R. Vounckx, "A hybridized optical thyristor-CMOS receiver for optoelectronic applications," *IEEE Photon. Technol. Lett.*, vol. 9, pp. 669–671, May 1997.
- [3] H. J. Kim, D. M. Kim, D. H. Woo, S. I. Kim, S. H. Kim, J. I. Lee, K. N. Kang, and K. Cho, "High photoresponsivity of a p-channel InGaP/GaAs/InGaAs double heterojunction pseudomorphic modulation-doped field effect transistor," *Appl. Phys. Lett.*, vol. 72, no. 5, pp. 584–586, 1998.
- [4] L. E. M. de Barros, Jr., A. Paoletta, M. Y. Frankel, M. A. Romero, P. R. Herczfeld, and A. Madjar, "Photoresponse of microwave transistors to high-frequency modulated lightwave carrier signal," *IEEE Trans. Microwave Theory Tech.*, vol. 45, pp. 1368–1374, Aug. 1997.
- [5] S. H. Song, D. M. Kim, H. J. Kim, S. H. Kim, K. N. Kang, and M. I. Nathan, "Photonic microwave characteristics and modeling of an $\text{Al}_{0.3}\text{Ga}_{0.7}\text{As}/\text{GaAs}/\text{In}_{0.13}\text{Ga}_{0.87}\text{As}$ double heterostructure pseudomorphic HEMT," *IEEE Microwave Guided Wave Lett.*, vol. 8, pp. 35–37, Jan. 1998.
- [6] J. P. Noad, E. H. Hara, R. H. Hum, and R. I. MacDonald, "FET photodetectors: A combined study using optical and electron-beam stimulation," *IEEE Trans. Electron Devices*, vol. ED-29, pp. 1792–1797, Nov. 1982.
- [7] K. Lee, M. S. Shur, T. J. Drummond, and H. Morkoc, "Parasitic MESFET in (Al,Ga)As/GaAs modulation doped FET's and MODFET characterization," *IEEE Trans. Electron Devices*, vol. ED-31, pp. 29–35, Jan. 1984.
- [8] D. Xu, H. Heib, S. Kraus, M. Sexl, G. Bohm, G. Trankle, G. Weimann, and G. Abstreiter, "High-performance double-modulation-doped InAlAs/InGaAs/InAs HFET's," *IEEE Electron Device Lett.*, vol. 18, pp. 323–325, July 1997 (see Fig. 2 for $V_{GS} = 0.5, 0.25, \text{ and } 0 \text{ V}$).